

Compressive ghost imaging

Ori Katz,^{a)} Yaron Bromberg, and Yaron Silberberg

Department of Physics of Complex Systems, The Weizmann Institute of Science, Rehovot 76100, Israel

(Received 10 May 2009; accepted 8 September 2009; published online 30 September 2009)

We describe an advanced image reconstruction algorithm for pseudothermal ghost imaging, reducing the number of measurements required for image recovery by an order of magnitude. The algorithm is based on *compressed sensing*, a technique that enables the reconstruction of an N -pixel image from much less than N measurements. We demonstrate the algorithm using experimental data from a pseudothermal ghost-imaging setup. The algorithm can be applied to data taken from past pseudothermal ghost-imaging experiments, improving the reconstruction's quality. © 2009 American Institute of Physics. [doi:10.1063/1.3238296]

Ghost imaging (GI) has emerged a decade ago as an imaging technique that exploits the quantum nature of light, and has been in the focus of many studies since.¹ In GI, an object is imaged even though the light which illuminates it is collected by a single-pixel detector which has no spatial resolution (a bucket detector). This is done by correlating the intensities measured by the bucket detector with the images of the light field which impinges upon the object. GI was originally performed using entangled photon pairs,² and later on was realized with classical light sources.³⁻⁶ The demonstrations of GI with classical light sources, and especially pseudothermal sources, triggered an ongoing effort to implement GI for various sensing applications.^{4,7} However, one of the main drawbacks of pseudothermal GI is the long acquisition times required for reconstructing images with a good signal-to-noise ratio (SNR).^{1,8}

In this work, we propose an advanced reconstruction algorithm for pseudothermal GI, which reduces significantly the required acquisition times. The algorithm is based on *compressed sensing* (or *compressive sampling*, CS),^{9,10} an advanced sampling and reconstruction technique which has been recently implemented in several fields of imaging. Examples for such are magnetic resonance imaging,¹¹ astronomy,¹² terahertz imaging,¹³ and single-pixel cameras.¹⁴ The main idea behind CS is to exploit the redundancy in the structure of most natural signals/objects to reduce the number of measurements required for faithful reconstruction. Here we show that applying a CS-based reconstruction algorithm to data taken from conventional pseudothermal GI measurements dramatically improves the SNR of the reconstructed images and thus allows for shorter acquisition times.

In conventional pseudothermal GI, an object is illuminated by a speckle field generated by passing a laser beam through a rotating diffuser [Fig. 1(a)]. For each phase realization r of the diffuser, the speckle field $I_r(x, y)$, which impinges on the object is imaged. This is done by splitting the beam before the object to an "object arm" and a "reference arm," and placing a charge coupled device (CCD) camera at the reference arm. At the object arm, a bucket detector measures the total intensity B_r that is transmitted through the object, represented by a transmission function $T(x, y)$,

$$B_r = \int dx dy I_r(x, y) T(x, y). \quad (1)$$

To reconstruct the object's transmission function $T(x, y)$, the bucket detector measurements are cross correlated with the intensity patterns measured at the reference arm,

$$T_{\text{GI}}(x, y) = \frac{1}{M} \sum_{r=1}^M (B_r - \langle B \rangle) I_r(x, y), \quad (2)$$

where $\langle \cdot \rangle \equiv \frac{1}{M} \sum_r$ denotes an ensemble average over M realizations (measurements). From Eq. (2) one can see that the image is obtained by a linear superposition of the intensity patterns $I_r(x, y)$ with the appropriate weights $B_r - \langle B \rangle$. Each bucket measurement B_r is the overlap between the object and the illumination pattern [Eq. (1)]. Thus, the GI measurement process is in essence a vector projection of the object transmission function $T(x, y)$ over M different random vectors $I_r(x, y)$.

The GI linear reconstruction process has no assumptions on the to-be-resolved object. Thus if the number of resolution cells (speckles) which cover the object is N , one needs

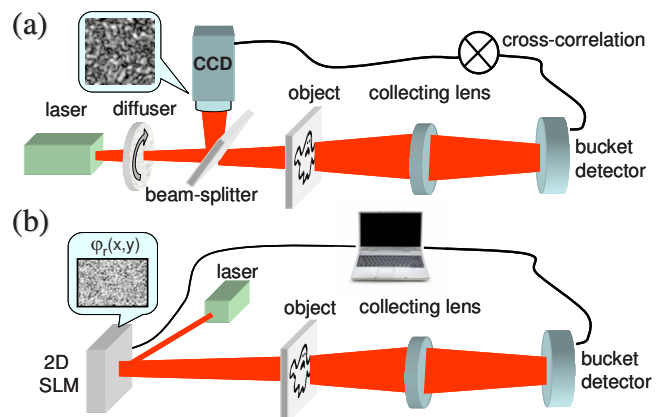


FIG. 1. (Color online) (a) Standard pseudothermal GI two-detectors setup. A copy of the speckle field which impinges on the object is imaged with a CCD camera, and correlated with the intensity measured by a bucket detector. (b) The computational GI single-detector setup used in this work. A pseudothermal light beam is generated by applying controllable random phase masks $\varphi_r(x, y)$ with a spatial light modulator. The object image is obtained by correlating the intensities measured by the bucket detector, with the *calculated* field at the object plane.

^{a)}Electronic mail: ori.katz@weizmann.ac.il.

at least $M=N$ different intensity patterns in order to reconstruct the object (the measurement's Nyquist limit). In fact, since the different intensity patterns $I_r(x,y)$ overlap, $M \gg N$ measurements are needed to meet $\text{SNR} \gg 1$.^{8,1} However, any prior information on the structure of the object could significantly reduce the number of measurements required for a faithful reconstruction. Remarkably, for most imaging tasks such information exists: natural images are sparse, that is, they contain many coefficients close to or equal to zero when represented in an appropriate basis [e.g., the two dimensional (2D) discrete cosine transform (DCT)]. This fact is at the core of modern lossy image compression algorithms, such as JPEG.¹⁰ The main idea behind CS is to exploit this sparsity/compressibility to reduce the number of measurements needed for faithful image recovery.

CS reconstruction algorithms search for the most sparse image in the compressible basis which fulfills the $M < N$ random projections measured. It requires solving a convex optimization program, seeking for the image $T_{\text{CS}}(x,y)$ which minimizes the L_1 -norm in the sparse basis (i.e., minimizes the sum of the absolute values of the transform coefficients),^{9,10}

$$T_{\text{CS}} = T' \text{ which minimizes: } \|\Psi\{T'(x,y)\}\|_{L_1},$$

$$\text{subject to } \int dx dy I_r(x,y) T'(x,y) = B_r \quad \forall r=1..M, \quad (3)$$

where B_r are the M gathered projections measurements and Ψ is the transform operator to the sparse basis [e.g., 2D-DCT]. Finding the image with the minimal L_1 -norm can be realized as a linear program, for which efficient solution methods exist. According to CS theory, one can reconstruct compressible images characterized by K transform coefficients with high fidelity, using just $M \geq O[K \log(N/K)]$ random measurements, where N is the total number of resolution cells in the image. Reconstruction of natural images using CS was demonstrated using $M \leq N/2$ measurements.^{10,11,14} This sub-Nyquist acquisition results from exploiting the image natural sparsity. We note that since the vectors $I_r(x,y)$ are random, they are most likely linearly independent and therefore $M \geq N$ projection-measurements span the image dimensionality. Thus, the image can be reconstructed (without exploiting the image sparsity) by solving a set of M linear equations using conventional linear least-squares methods. Such a linear algebra based reconstruction outperforms the standard GI reconstruction when $M \geq N$, and gives a perfect result in the absence of measurement noise.

To experimentally demonstrate CS reconstruction in GI, we have used the computational GI setup presented in Ref. 15 [Fig. 1(b)]. Computational GI is a variant of the standard two-detectors pseudothermal GI, where the rotating diffuser is replaced by a computer controlled spatial light modulator (SLM).¹⁶ Knowing the applied SLM phase mask for each realization $\varphi_r(x,y)$, the intensity of the field at the reference arm $I_r(x,y)$ is computed using the Fresnel-Huygens propagator, instead of it being measured as in conventional GI. It is important to note that CS reconstruction can be applied to any form of pseudothermal GI. It makes no difference if the reference intensity patterns are computed or measured.

The reconstruction results for a double slit transmission plate (width 220 μm , separation 500 μm), using $M=256$

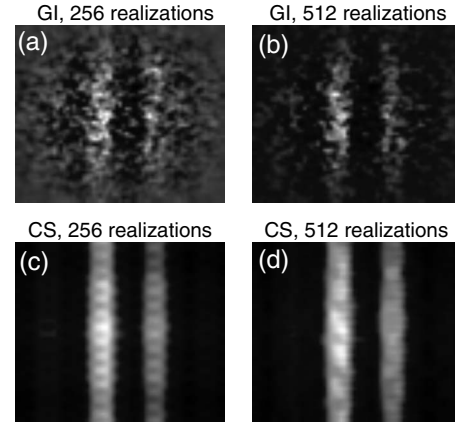


FIG. 2. Experimental reconstruction of a double-slit transmission plate. Top panel: conventional GI reconstruction with 256 realizations (a) and 512 realizations (b). Bottom panel [(c) and (d)]: CS reconstruction using the same experimental data as in (a) and (b). The increase in SNR using CS reconstruction is by a factor of 4.4 in (c) and 4.0 in (d).

and $M=512$ realizations are summarized in Fig. 2. The results of conventional GI reconstruction are plotted in Figs. 2(a) and 2(b), and the CS reconstructions using the same set of measured data are plotted in Figs. 2(c) and 2(d). To quantify the improvement gained by utilizing CS reconstruction, we have calculated the mean SNR of the reconstructed images. The signal was taken as the difference between the mean intensity of the bright slit and the dark background, and the noise was taken as the standard deviation of the dark background pixels. The calculated SNR for the CS reconstruction using 256 realizations is 4.4 times higher than for the standard GI reconstruction, and is 4.0 times higher in the 512 realizations case. Since the SNR in conventional GI scales as the square-root of the number of realizations,^{1,8} our results imply that CS allows for an order of magnitude faster image acquisition, making it attractive for practical imaging tasks. The reconstructions fidelity was estimated by calculating the mean-square error (MSE) of the reconstructions compared to a reference image T_{ref} , measured directly by a transmission microscope. The MSE given by $\frac{1}{N_{\text{pix}}} \sum_{i,j} [T_{\text{CS/GI}}(x_i, y_j) - T_{\text{ref}}(x_i, y_j)]^2$ is 0.12 for GI and 0.04 for CS using 512 realizations and 0.14 for GI and 0.05 for CS using 256 realizations. The summation is done over all the image pixels N_{pix} .

The pixel-resolution of the calculated speckle-field image $I_r(x,y)$ used for the reconstructions was 64×64 pixels ($N_{\text{pix}}=4096$). At this resolution, the speckles full width at half maximum (FWHM) was 1.53 pixels, yielding $N=1750$ resolution cells covering the object. This sets the measurement's Nyquist limit. Therefore in Figs. 2(a) and 2(c) the number of measurements used for the reconstructions is 15% of the Nyquist limit. In Figs. 2(b) and 2(d) the number of measurements is 30% of the Nyquist limit. The pixel resolution was chosen such that the individual speckles are resolved (pixel size < speckle size), yet the required computational resources are minimized. For the CS reconstruction we have utilized the gradient projection for sparse reconstruction algorithm,¹⁷ minimizing the L_1 -norm in the 2D-DCT domain. This algorithm follows Eq. (3), but considers the presence of noise in each measurement B_r , by relaxing the equality constraint.

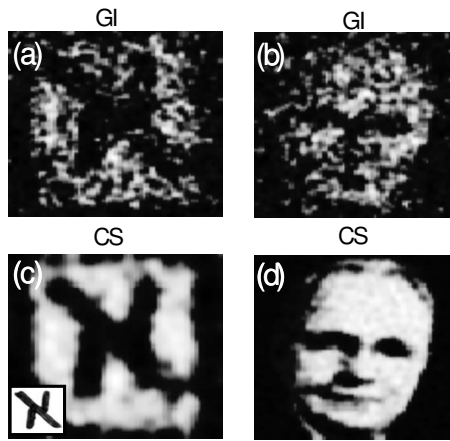


FIG. 3. (a) Experimental GI reconstruction of a transmission plate of the Hebrew letter Aleph (\aleph) from 1024 measurements. (c) Same as (a) but utilizing CS reconstruction, yielding 3.5 times higher SNR. (Inset: the object's transmission image). [(b) and (d)] Simulated GI and CS reconstructions of a 70×76 pixels grayscale portrait of H. Nyquist, using 800 measurements (60% the Nyquist limit).

To verify the applicability of CS reconstruction for more general images, we have imaged a transmission plate of the Hebrew letter Aleph (\aleph). The results for both GI and CS reconstructions using the same set of 1024 measurements are presented in Figs. 3(a) and 3(c). The reference data size used in this case was 70×76 pixels, and the speckles size was 2.01 pixels FWHM ($N=1330$). The calculated SNR for the CS reconstruction was 3.5 times higher than the GI SNR, and the calculated MSE was 0.05 with CS reconstruction and 0.1 with GI reconstruction. Finally, we demonstrate sub-Nyquist CS-GI reconstruction of a natural grayscale image, by reconstructing a 76×70 pixel image, containing $N=1330$ resolution cells from 800 simulated measurements, obtained by multiplying the speckle patterns used in the Aleph reconstruction experiment by the grayscale image values. The obtained MSE is 0.09 for the GI reconstruction and 0.005 for the CS reconstruction [Figs. 3(b) and 3(d)].

In conclusion, we have shown that by employing notions from CS theory in a GI reconstruction algorithm, one can boost the recovered image quality. CS unleashes the full po-

tential of the random projections measurement process of pseudothermal GI. It enables image reconstruction with far less measurements than is possible with conventional GI, and in some scenarios, with a scanning beam imaging setup. CS therefore holds potential for future implementations of GI in practical applications such as LIDAR. The presented algorithm can be applied to any pseudothermal GI data taken in the past, yielding superior reconstruction. Moreover, since computational GI allows for scanning-less three-dimensional (3D) image reconstruction,^{15,16} one may consider applying CS-GI to reconstruct 3D objects utilizing sparsity in the 3D-DCT domain or any other 3D-sparse transform basis.

We thank Igor Carron, Justin Romberg, Amnon Amir, and Dror Baron for helpful discussions and KFC and Wim for the arXiv blog thread.

- ¹A. Gatti, M. Bache, D. Magatti, E. Brambilla, F. Ferri, and L. A. Lugiato, *J. Mod. Opt.* **53**, 739 (2006).
- ²T. B. Pittman, Y. H. Shih, D. V. Strekalov, and A. V. Sergienko, *Phys. Rev. A* **52**, R3429 (1995).
- ³R. S. Bennink, S. J. Bentley, and R. W. Boyd, *Phys. Rev. Lett.* **89**, 113601 (2002).
- ⁴J. Cheng and S. Han, *Phys. Rev. Lett.* **92**, 093903 (2004).
- ⁵F. Ferri, D. Magatti, A. Gatti, M. Bache, E. Brambilla, and L. A. Lugiato, *Phys. Rev. Lett.* **94**, 183602 (2005).
- ⁶A. Valencia, G. Scarcelli, M. D'Angelo, and Y. Shih, *Phys. Rev. Lett.* **94**, 063601 (2005).
- ⁷R. Meyers, K. S. Deacon, and Y. Shih, *Phys. Rev. A* **77**, 041801(R) (2008).
- ⁸B. I. Erkmen and J. H. Shapiro, *Phys. Rev. A* **79**, 023833 (2009).
- ⁹E. J. Candes, and M. B. Wakin, *IEEE Signal Process. Mag.* **25**, 21 (2008).
- ¹⁰J. Romberg, *IEEE Signal Process. Mag.* **25**, 14 (2008).
- ¹¹M. Lustig, D. Donoho, and J. M. Pauly, *Magn. Reson. Med.* **58**, 1182 (2007).
- ¹²J. Bobin, J. L. Starck, and R. Ottensamer, *IEEE J. Sel. Top. Signal Process.* **2**, 718 (2008).
- ¹³W. L. Chan, K. Charan, D. Takhar, K. F. Kelly, R. G. Baraniuk, and D. M. Mittleman, *Appl. Phys. Lett.* **93**, 121105 (2008).
- ¹⁴M. F. Duarte, M. A. Davenport, D. Takhar, J. N. Laske, T. Sun, K. F. Kelly, and R. G. Baraniuk, *IEEE Signal Process. Mag.* **25**, 83 (2008).
- ¹⁵Y. Bromberg, O. Katz, and Y. Silberberg, *Phys. Rev. A* **79**, 053840 (2009).
- ¹⁶J. H. Shapiro, *Phys. Rev. A* **78**, 061802(R) (2008).
- ¹⁷M. A. T. Figueiredo, R. D. Nowak, and S. J. Wright, *IEEE J. Sel. Top. in Sig., Proc.* **1**, 586 (2007).